

12-27-99

A

PATENT

Attorney Docket No. MASIMO.149A

Date: December 23, 1999

Page 1

12/23/99  
JCS520 U.S. PTO

JCS584 U.S. PTO  
09/471510  
12/23/99

ASSISTANT COMMISSIONER FOR PATENTS

WASHINGTON, D.C. 20231

ATTENTION: BOX PATENT APPLICATION

Sir:

Transmitted herewith for filing is the patent application of

Inventors: **Mohamed K. Diab**

For: **PLETHYSMOGRAPH PULSE RECOGNITION PROCESSOR**

Enclosed are:

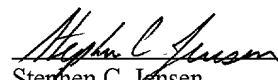
- (X) 19 sheets of drawings.
- (X) Return prepaid postcard.

CLAIMS AS FILED

FOR	NUMBER FILED	NUMBER EXTRA	RATE	FEE
Basic Fee			\$760	\$760
Total Claims	17 - 20 =	0 ×	\$18	\$0
Independent Claims	3 - 3 =	0 ×	\$78	\$0
If application contains any multiple dependent claims(s), then add			\$260	\$0

**FILING FEE TO BE PAID** \$760  
**AT A LATER DATE**

- (X) Please use Customer No. 20,995 for the correspondence address.

  
 Stephen C. Jensen  
 Registration No. 35,556  
 Attorney of Record

H:\DOCS\SCJ\SCJ-2437.DOC  
 122299

INTELLECTUAL PROPERTY LAW  
KNOBBE, MARTENS, OLSON & BEAR

A LIMITED LIABILITY PARTNERSHIP INCLUDING  
PROFESSIONAL CORPORATIONS  
PATENT, TRADEMARK AND COPYRIGHT CAUSES  
620 NEWPORT CENTER DRIVE  
SIXTEENTH FLOOR  
NEWPORT BEACH, CALIFORNIA 92660-8016  
(949) 760-0404  
FAX (949) 760-9502  
INTERNET WWW.KNOB.COM

LOUIS J. KNOBBE\*  
DON W. MARTENS\*  
GORDON H. OLSON\*  
JAMES B. BEAR  
DARRELL L. OLSON\*  
WILLIAM B. BUNKER  
WILLIAM H. NIEMAN  
LOWELL ANDERSON  
ARTHUR S. ROSE  
JAMES F. LESNIAK  
NED A. ISRAELSEN  
DREW S. HAMILTON  
JERRY T. SEWELL  
JOHN B. SGANGA, JR  
EDWARD A. SCHLATTER  
GERARD VON HOFFMANN  
JOSEPH R. RE  
CATHERINE J. HOLLAND  
JOHN M. CARSON  
KAREN VOGEL WEIL  
ANDREW H. SIMPSON  
JEFFREY L. VAN HOUSEAR  
DANIEL E. ALTMAN  
ERNEST A. BEUTLER  
MARGUERITE L. GUNN  
STEPHEN C. JENSEN  
VITO A. CANUSO III  
WILLIAM H. SHREVE  
LYNDA J. ZADRA-SYMES†  
STEVEN J. NATAUPSKY  
PAUL A. STEWART  
JOSEPH F. JENNINGS  
CRAIG S. SUMMERS  
ANNEMARIE KAISER

BRENTON R. BABCOCK  
THOMAS F. SMEGAL, JR.  
MICHAEL H. TRENHOLM  
DIANE M. REED  
JONATHAN A. BARNEY  
RONALD J. SCHOENBAUM  
JOHN R. KING  
FREDERICK S. BERRETTA  
NANCY WAYS VENSKE  
JOHN P. GIEZENTANNER  
ADEEL S. AKHTAR  
GINGER R. DREGER  
THOMAS R. ARNO  
DAVID N. WEISS  
DANIEL HART, PH.D.  
DOUGLAS G. MUEHLHAUSER  
LORI LEE YAMATO  
STEPHEN M. LOBBIN  
ROBERT F. GAZDZINSKI  
STACEY R. HALPERN  
MICHAEL K. FRIEDLAND  
DALE C. HUNT, PH.D.  
LEE W. HENDERSON, PH.D.  
DEBORAH S. SHEPHERD  
RICHARD E. CAMPBELL  
MARK M. ABUMERI  
JON W. GURKA  
KATHERINE W. WHITE  
ERIC M. NELSON  
ALEXANDER C. CHEN  
MARK R. BENEDICT, PH.D.  
PAUL N. CONOVER  
ROBERT J. ROBY  
SABING H. LEE

KAROLINE A. DELANEY  
JOHN W. HOLCOMB  
JAMES J. MULLEN, III, PH.D.  
JOSEPH S. CIANFRANI  
JOSEPH M. REISMAN, PH.D.  
WILLIAM R. ZIMMERMAN  
GLEN L. NUTTALL  
ERIC S. FURMAN, PH.D.  
DO TE KIM  
TIRZAH ABE LOWE  
GEOFFREY Y. IIDA  
ALEXANDER S. FRANCO  
SANJIVPAL S. GILL  
SUSAN M. MOSS  
JAMES W. HILL, M.D.  
ROSE M. THIESSEN, PH.D.  
MICHAEL L. FULLER  
MICHAEL A. GUILIANA  
MARK J. KERTZ  
RABINDER N. NARULA  
BRUCE S. ITCHKAWITZ, PH.D.  
PETER M. MIDGLEY  
THOMAS S. MCCLLENANAH  
MICHAEL S. OKAMOTO  
M. CHRISTINA THOMSON  
JOHN M. GROVER  
MALLARY K. MCCARTHY  
IRFAN A. LATEEF  
AMY C. CHRISTENSEN  
SHARON S. NG  
MARK J. GALLAGHER  
DAVID G. JANKOWSKI, PH.D.  
BRIAN C. HORNE  
PAYSON J. LEMEILLEUR

OF COUNSEL  
JERRY R. SEILER  
JAPANESE PATENT ATTY  
KATSUHIRO ARAI\*\*  
EUROPEAN PATENT ATTY  
MARTIN HELLEBRANDT  
KOREAN PATENT ATTY  
MINCHEOL KIM  
SCIENTISTS & ENGINEERS  
(NON-LAWYERS)  
RAIMOND J. SALENIKS\*\*  
NEIL S. BARTFELD, PH.D.\*\*  
DANIEL E. JOHNSON, PH.D.\*\*  
JEFFERY KOEPKE, PH.D.  
KHURRAM RAHMAN, PH.D.  
JENNIFER A. HAYNES, PH.D.  
BRENDAN P. O'NEILL, PH.D.  
THOMAS Y. NAGATA  
ALAN C. GORDON  
PABLO S. HUERTA  
LINDA H. LIU  
MICHAEL J. HOLIHAN  
YASHWANT VAISHNAV, PH.D.  
MEGUMI TANAKA

Assistant Commissioner for Patents  
Washington, D.C. 20231


**CERTIFICATE OF MAILING BY "EXPRESS MAIL"**

**Attorney Docket No. :** MASIMO.149A  
**Applicant(s) :** Mohamed K. Diab  
**For :** PLETHYSMOGRAPH PULSE RECOGNITION  
PROCESSOR  
**Attorney :** Stephen C. Jensen  
**"Express Mail"**  
**Mailing Label No. :** EL207463935  
**Date of Deposit :** December 23, 1999

I hereby certify that the accompanying

Transmittal in Duplicate; Specification in 18 pages; 19 sheets of drawings; Return  
Prepaid Postcard

are being deposited with the United States Postal Service "Express Mail Post Office to Addressee"  
service under 37 CFR 1.10 on the date indicated above and are addressed to the Assistant Commissioner  
for Patents, Washington, D.C. 20231.

  
Arthur Greene

H:\DOCS\SCJ\SCJ-2439.DOC  
122299

201 CALIFORNIA STREET  
SUITE 1150  
SAN FRANCISCO, CALIFORNIA 94111  
(415) 954-4114  
FAX (415) 954-4111

501 WEST BROADWAY  
SUITE 1400  
SAN DIEGO, CALIFORNIA 92101-3505  
(619) 235-8550  
FAX (619) 235-0176

3801 UNIVERSITY AVENUE  
SUITE 710  
RIVERSIDE, CALIFORNIA 92501  
(909) 781-9231  
FAX (909) 781-4507

\* A PROFESSIONAL CORPORATION  
† ALSO BARRISTER AT LAW (U.K.)  
\*\* U.S. PATENT AGENT

**PLETHYSMOGRAPH PULSE RECOGNITION PROCESSOR**Background of the Invention

Oximetry is the measurement of the oxygen status of blood. Early detection of low blood oxygen is critical in the medical field, for example in critical care and surgical applications, because an insufficient supply of oxygen can result in brain damage and death in a matter of minutes. Pulse oximetry is a widely accepted noninvasive procedure for measuring the oxygen saturation level of arterial blood, an indicator of oxygen supply. A pulse oximeter typically provides a numerical readout of the patient's oxygen saturation, a numerical readout of pulse rate, and an audible indicator or "beep" that occurs at each pulse.

A pulse oximetry system consists of a sensor attached to a patient, a monitor, and a cable connecting the sensor and monitor. Conventionally, a pulse oximetry sensor has both red and infrared (IR) light-emitting diode (LED) emitters and a photodiode detector. The sensor is typically attached to an adult patient's finger or an infant patient's foot. For a finger, the sensor is configured so that the emitters project light through the fingernail and into the blood vessels and capillaries underneath. The photodiode is positioned at the fingertip opposite the fingernail so as to detect the LED emitted light as it emerges from the finger tissues.

The pulse oximetry monitor (pulse oximeter) determines oxygen saturation by computing the differential absorption by arterial blood of the two wavelengths emitted by the sensor. The pulse oximeter alternately activates the sensor LED emitters and reads the resulting current generated by the photodiode detector. This current is proportional to the intensity of the detected light. The pulse oximeter calculates a ratio of detected red and infrared intensities, and an arterial oxygen saturation value is empirically determined based on the ratio obtained. The pulse oximeter contains circuitry for controlling the sensor, processing the sensor signals and displaying the patient's oxygen saturation and pulse rate. In addition, a pulse oximeter may display the patient's plethysmograph waveform, which is a visualization of blood volume change in the illuminated tissue

caused by arterial blood flow over time. A pulse oximeter is described in U.S. Patent No. 5,632,272 assigned to the assignee of the present invention.

### Summary of the Invention

5           FIG. 1 illustrates the standard plethysmograph waveform **100**, which can be derived from a pulse oximeter. The waveform **100** is a display of blood volume, shown along the y-axis **110**, over time, shown along the x-axis **120**. The shape of the plethysmograph waveform **100** is a function of heart stroke volume, pressure gradient, arterial elasticity and peripheral resistance. The ideal waveform **100** displays a broad  
10           peripheral flow curve, with a short, steep inflow phase **130** followed by a 3 to 4 times longer outflow phase **140**. The inflow phase **130** is the result of tissue distention by the rapid blood volume inflow during ventricular systole. During the outflow phase **140**, blood flow continues into the vascular bed during diastole. The end diastolic baseline **150** indicates the minimum basal tissue perfusion. During the outflow phase **140** is a dicrotic notch **160**, the nature of which is disputed. Classically, the dicrotic notch **160** is attributed to closure of the aortic valve at the end of ventricular systole. However, it may also be the result of reflection from the periphery of an initial, fast propagating, pressure pulse that occurs upon the opening of the aortic valve and that precedes the arterial flow wave. A double dicrotic notch can sometimes be observed, although its explanation is obscure,  
15           possibly the result of reflections reaching the sensor at different times.  
20

          FIG. 2 is a graph **200** illustrating the absorption of light at a tissue site illuminated by a pulse oximetry sensor. The graph **200** has a y-axis **210** representing the total amount of light absorbed by the tissue site, with time shown along an x-axis **220**. The total absorption is represented by layers, including the static absorption layers due to tissue **230**,  
25           venous blood **240** and a baseline of arterial blood **250**. Also shown is a variable absorption layer due to the pulse-added volume of arterial blood **260**. The profile **270** of the pulse-added arterial blood **260** is seen as the plethysmograph waveform **100** depicted in FIG. 1.

          FIG. 3 illustrates the photo-plethysmograph intensity signal **300** detected by a  
30           pulse oximeter sensor. A pulse oximeter does not directly detect absorption and, hence,

does not directly measure the standard plethysmograph waveform 100 (FIG. 1). However, the standard plethysmograph can be derived by observing that the detected intensity signal 300 is merely an out of phase version of the absorption profile 270. That is, the peak detected intensity 372 occurs at minimum absorption 272 (FIG. 2), and the minimum detected intensity 374 occurs at maximum absorption 274 (FIG. 2). Further, a rapid rise in absorption 276 (FIG. 2) during the inflow phase of the plethysmograph is reflected in a rapid decline 376 in intensity, and the gradual decline 278 (FIG. 2) in absorption during the outflow phase of the plethysmograph is reflected in a gradual increase 378 in detected intensity.

In addition to blood oxygen saturation, a desired pulse oximetry parameter is the rate at which the heart is beating, i.e. the pulse rate. At first glance, it seems that it is an easy task to determine pulse rate from the red and infrared plethysmograph waveforms described above. However, this task is complicated, even under ideal conditions, by the variety of physiological plethysmographic waveforms. Further, plethysmographic waveforms are often corrupted by noise, including motion artifact, as described in U.S. Patent No. 2,632,272 cited above. Plethysmograph pulse recognition, especially in the presence of motion artifact and other noise sources, is a useful component for determining pulse rate and also for providing a visual or audible indication of pulse occurrence.

In one aspect of the pulse recognition processor according to the present invention, information regarding pulses within an input plethysmograph waveform is provided at a processor output. The processor has a candidate pulse portion that determines a plurality of potential pulses within the input waveform. A physiological model portion of the processor then determines the physiologically acceptable ones of these potential pulses. The processor may further provide statistics regarding the acceptable pulses. One statistic is pulse density, which is the ratio of the period of acceptable pulses to the duration of an input waveform segment.

The candidate pulse portion has a series of components that remove from consideration as potential pulses those waveform portions that do not correspond to an idealized triangular waveform. This processing removes irrelevant waveform features

such as the characteristic dicrotic notch and those caused by noise or motion artifact. The candidate pulse portion provides an output having indices that identify potential pulses relative to the peaks and valleys of this triangular waveform.

5 The physiological model portion of the processor has a series of components that discard potential pulses that do not compare to a physiologically acceptable pulse. The first component of the model portion extracts features of the potential pulses, including pulse starting point, pulse period, and pulse signal strength. These features are compared against various checks, including checks for pulses that have a period below a predetermined threshold, that are asymmetric, that have a descending trend that is  
10 generally slower than a subsequent ascending trend, that do not sufficiently comply with an empirical relationship between pulse rate and pulse signal strength, and that have a signal strength that differs from a short-term average signal strength by greater than a predetermined amount.

In another aspect of the present invention, a pulse recognition method includes  
15 the steps of identifying a plurality of potential pulses in an input waveform and comparing the potential pulses to a physiological pulse model to derive at least one physiologically acceptable pulse. A further step of generating statistics for acceptable pulses may also be included. The generating step includes the steps of determining a total period of acceptable pulses and calculating a ratio of this total period to a duration  
20 of an input waveform segment to derive a pulse density value. The comparing step includes the steps of extracting pulse features from potential pulses and checking the extracted features against pulse criteria.

Yet another aspect of the current invention is a pulse recognition processor having a candidate pulse means for identifying potential pulses in an input waveform  
25 and providing a triangular waveform output. The processor also has a plethysmograph model means for determining physiologically acceptable pulses in the triangular waveform output and providing as a pulse output the indices of acceptable pulses. The pulse recognition processor may further have a pulse statistics means for determining cumulative pulse characteristics from said pulse output.

### Brief Description of the Drawings

The present invention will be described in detail below in connection with the following drawing figures in which:

FIG. 1 is a graph illustrating a single pulse of a plethysmograph waveform;

5        FIG. 2 is a graph illustrating the absorption contribution of various blood and tissue components;

FIG. 3 is a graph illustrating an intensity “plethysmograph” pulse oximetry waveform;

10       FIG. 4 is a block diagram of the plethysmograph pulse recognition processor according to the present invention;

FIG. 5 is a block diagram of the candidate pulse finding subprocessor portion of the present invention;

FIG. 6 is a graph illustrating the filtered, curvature of a plethysmograph pulse and the associated edges;

15       FIG. 7 is a graph illustrating the delta T check on the edges;

FIG. 8 is a graph illustrating the zero-crossing check on the edges;

FIG. 9 is a graph illustrating the amplitude threshold check on the edges;

FIG. 10 is a graph illustrating the max-min check on the edges;

FIG. 11 is a graph illustrating the output of the pulse finder;

20       FIG. 12 is a block diagram of the plethysmograph model subprocessor portion of the present invention;

FIG. 13 is a graph illustrating the parameters extracted by the pulse features component of the model subprocessor;

FIG. 14 is a graph illustrating the stick model check on the candidate pulses;

25       FIG. 15 is a graph illustrating an angle check on the candidate pulses;

FIG. 16 is a graph illustrating a pulse that would be discarded by the angle check;

FIG. 17 is a graph illustrating a pulse that would be discarded by the ratio check;

FIG. 18 is a graph illustrating one test of the signal strength check; and

30       FIG. 19 is a block diagram of a pulse rate selection and comparison module in accordance with a preferred embodiment of the present invention.

### Detailed Description of the Preferred Embodiments

FIGS. 4 illustrates the plethysmograph pulse recognition processor 400 according to the present invention. The pulse processor 400 has three subprocessors, a candidate pulse subprocessor 410, a plethysmograph model subprocessor 460, and a pulse statistics subprocessor 490. The candidate pulse subprocessor 410 applies various waveform criteria or “edge checks” to find candidate pulses in an input waveform “snapshot” 412. In a particular embodiment, the snapshot is 400 samples of a detected intensity plethysmograph taken at a 62.5 Hz sampling rate. This snapshot represents a 6.4 second waveform segment. The output 414 of the candidate pulse subprocessor 410 is peaks and valleys of the input waveform segment representing a triangular wave model of identified candidate pulses. The candidate pulse output 414 is input to the plethysmograph model subprocessor 460, which compares these candidate pulses to an internal model for physiological pulses. The output 462 of the plethysmograph model subprocessor 460 is physiologically acceptable pulses. The acceptable pulse output 462 is input to the pulse statistics subprocessor. The output 492 of the pulse statistics subprocessor is statistics regarding acceptable pulses, including mean pulse period and pulse density, as described below.

FIG. 5 illustrates the components of the candidate pulse subprocessor 410. This subprocessor removes waveform features that do not correspond to an idealized triangular waveform, including the characteristic dicrotic notch. For example, as shown in FIG. 3, the candidate pulse component must identify points ABE, discarding points CD. The candidate pulse subprocessor 410 first identifies “edges” within the input waveform segment. An edge is defined as a segment that connects a peak and subsequent valley of the differentiated waveform signal. The candidate pulse processor 410 then discards edges that do not meet certain conditions.

As shown in FIG. 5, the candidate pulse subprocessor has curvature 500, low-pass filter 510 and edge finder 520 components that identify edges. In one embodiment, the curvature component 510 is implemented by convolving the waveform with the kernel [1,-2,1]. This is followed by a low-pass filter:

$$y_k = w \dot{y}_{k-1} + u_k \quad (1)$$



where  $u_k$  is the  $k$ th input sample and  $y_k$  is the  $k$ th output sample and  $w$  is a fixed weight that determines the amount of filter feedback. The edge finder **520** identifies the peaks and subsequent valleys of the output of the filter **510**.

FIG. 6 illustrates the results of the curvature **500**, filter **510** and edge finder **520** components applied to a couple waveform pulses **610**. The processed waveform **660** has peaks A and C and corresponding valleys B and D. There are two edges, a first edge is represented by a line segment **670** connecting A and B. A second edge is represented by a line segment **680** connecting C and D.

As shown in FIG. 5, the candidate pulse portion also has delta T **530**, zero crossing **540**, amplitude threshold **550** and max-min **560** checks that eliminate certain of the identified edges. The delta T check **530** discards all the edges having a distance between end points that do not fall within a fixed interval. This is designed to eliminate pulse-like portions of the input waveform that are either too slow or too quick to be physiological pulses. In a particular embodiment, the interval is between 5 and 30 samples at the 62.5 Hz sampling rate, or 80-480 msec. That is, edges less than 80 msec. or greater than 480 msec. in length are eliminated.

FIG. 7 illustrates the delta T check **530** (FIG. 5) described above. Shown is the processed waveform **760**, edge *a* **780** and edge *b* **790**, along with a maximum acceptable edge length interval **770** for comparison. In this example, edge *a* **780**, which is 35 samples in length, would be eliminated as exceeding in length the maximum acceptable interval **770** of 30 samples. By contrast, edge *b* **790**, which is 25 samples in length, would be accepted.

Also shown in FIG. 5, the zero crossing check **540** eliminates all edges that do not cross zero. The zero crossing check eliminates small curvature changes in the input waveform segment, i.e. small bumps that are not peaks and valleys.

FIG. 8 illustrates the effect of the zero crossing check **540** (FIG. 5). Shown is the processed waveform **860**. Edge *a* **870**, edge *b* **880** and edge *c* **890** are shown relative to the zero line **865** for the processed waveform **860**. In this example, edges *a* **870** and edge *b* **880** are accepted, but edge *c* **890** is eliminated because it does not cross the zero line **865**.

Shown in FIG. 5, the amplitude threshold check **550** is designed to remove larger “bumps” than the zero crossing check **540**, such as dicrotic notches. This is done by comparing the right extreme (valley) of each edge within a fixed-length window to a threshold based on a fixed percentage of the minimum within that window. If the valley is not sufficiently deep, the edge is rejected. In a particular embodiment, the window size is set at 50 samples for neonates and 100 samples for adults in order accommodate the slower pulse rate of an adult. Also, a threshold of 60% of the minimum is used.

FIG. 9 illustrates an example of the amplitude threshold check **550** (FIG. 5). Shown is a the processed waveform **960**. The starting point of the window **970** is set to the left extreme **942** (peak) of the first edge *a*. A minimum **980** within the window **970** is determined. A threshold **982** equal to 60% of the minimum **980** is determined. The right extreme **992** of edge *a* is compared with the threshold **982**. Edge *a* is kept because the right extreme **992** is smaller than (more negative) than the threshold **982**. The right extreme **993** of edge *b* is then compared with the threshold **982**. Edge *b* is removed because the right extreme **993** is greater than (less negative) than the threshold **982**. Similarly, edge *c* is kept. Next, the window **970** is moved to the left extreme **943** of edge *b* and the process repeated.

Also shown in FIG. 5, the max-min check **560** applies another removal criteria to the edges. The max-min check **560** considers the interval of the processed waveform between the minimum of an edge being checked and the peak of the subsequent edge. The max-min check **560** finds the maximum of the processed waveform within this interval. The edge being checked is removed if the maximum is greater than a percentage of the absolute value of the right extreme (minimum) of that edge. In one embodiment requiring the most stringent algorithm performance, the threshold is set to 77% of the right extreme of the edge. In another embodiment with less stringent algorithm performance, the threshold is set to 200% of the right extreme of the edge. The max-min check **560** is effective in eliminating edges that are pulse-like but correspond to motion.

FIG. 10 illustrates an example of the max-min check **560** (FIG. 5). Shown is the processed waveform **1060**. The max-min check **560** is applied to edge *b* **1070**. The

interval B-C is considered, which is between point B **1074**, the peak of edge *b* **1070**, and point C **1084**, the peak of edge *c* **1080**. The maximum in the interval B-C is point C **1084**. Point C **1084** is compared to a first threshold **1078**, which in this example is 77% of the absolute value of point P1 **1072**, the minimum of edge *b* **1070**. Edge *b* **1070** would not be discarded because point C **1084** is smaller than this first threshold **1078**. As another example, the max-min check **560** is applied to edge *c* **1080**. The interval C-D is considered, which is between point C **1084**, the peak of edge *c* **1080**, and point D **1094**, the peak of edge *d* **1090**. The maximum in the interval C-D is point V **1093**. Point V **1093** is compared to a second threshold **1088**, which is 77% of the absolute value of point P2 **1082**, the valley of edge *c* **1080**. Edge *c* would be discarded because point V **1093** is greater than this second threshold **1088**.

As shown in FIG. 5, the pulse finder **570** is the last component of the candidate pulse subprocessor **410**. The pulse finder **570** transforms the edges remaining after the various edge checks into candidate pulses in the form of an idealized triangular wave, which are fed into the plethysmograph model subprocessor **460** (FIG. 4). From the information about the indices of the peaks of valleys of the remaining edges, it is simple to determine a pulse in the input waveform. The remaining edges are first divided into edge pairs, i.e. the first and second edges, the second and third edges, and so on. The first point of a pulse corresponds to the maximum of the waveform segment in the interval of indices determined by the peak and valley of the first edge of a pair. The second point is the minimum between the valley of the first edge and the peak of the second edge. The third and last point is the maximum between the peak and the valley of the second edge.

FIG. 11 illustrates the result of the pulse finder **570** (FIG. 5) shown as a series of pulses **1110**, including a particular pulse XYZ **1120** appearing as a triangular wave superimposed on an input waveform segment **1140**. Also shown are the remaining edges *a* **1170**, *b* **1180** and *c* **1190**. In this example, pulse XYZ **1120** is formed from the pair of edges *c* **1180** and *e* **1190**. Point X **1122** is the maximum in the waveform segment **1140** in the time interval between the peak **1182** and valley **1184** of edge *c* **1180**. Point Y **1124** is the minimum in the waveform segment **1140** in the time interval

between the valley **1184** of edge *c* **1180** and the peak **1192** of edge *e* **1190**. Point Z **1128** is the maximum in the waveform segment **1140** in the time interval between the peak **1192** and valley **1194** of edge *e* **1190**.

FIG. **12** illustrates the components of the plethysmograph model subprocessor **460**. This subprocessor takes as input the candidate pulses identified by the candidate pulse subprocessor **410** (FIG. **4**) and decides which of these satisfies an internal model for a physiological plethysmographic waveform. Although the candidate pulse subprocessor **410** (FIG. **4**) performs a series of checks on edges, the plethysmograph model subprocessor performs a series of checks on pulse features. The first component of the model subprocessor calculates relevant pulse features. The remainder of the model subprocessor checks these pulse features to identify physiologically acceptable features.

Shown in FIG. **12**, the pulse features component **1210** extracts three items of information about the input candidate pulses that are needed for downstream processing by the other components of the model subprocessor. The extracted features are the pulse starting point, period and signal strength.

FIG. **13** illustrates a candidate pulse **1300** and the three parameters extracted by the pulse features component **1210** (FIG. **12**). The pulse **1300** is shown overlaid on the input waveform **1302** for reference. The starting point A **1360** is the first peak of the pulse **1300**. The period P **1370** is the time difference between the time of occurrence of the first peak **1360** and the second peak **1362** of the pulse **1300**. The signal strength SS **1350** is the difference between the values of the first peak **1360** and the valley **1364** of the pulse **1300**. The signal strength SS **1350** is normalized by dividing this value by the value of the infrared raw signal data at the point corresponding to point A **1360**.

Also shown in FIG. **12** is the 250 BPM check **1220**. This component discards pulses having a period P **1370** (FIG. **13**) that is below 15 samples. This corresponds to an upper limit for the pulse rate set at 250 beats per minute. That is:

$$15 \text{ samples/beat} = (62.5 \text{ samples/sec.} \times 60 \text{ sec./min.}) / 250 \text{ beats per min.} \quad (2)$$

In addition, FIG. **12** shows the stick model check **1230**. This component discards pulses where the corresponding waveform does not fit a stick model, i.e. where

a pulse cannot be represented by a triangular waveform. This component measures a normalized difference between the input waveform and the triangular wave representation of that waveform. The obtained value is compared to a threshold, and pulses are discarded where the normalized difference is greater than that threshold.

FIG. 14 illustrates the calculations performed by the stick model check 1230 (FIG. 12). Shown is an input waveform pulse 1410 and the corresponding stick model pulse 1460. The stick model check 1230 (FIG. 12) component computes a first value, which is a sum of the absolute differences, shown as the dark black areas 1420, between the waveform pulse 1410 and the stick model pulse 1460. This component also computes a second value, which is a sum of the first rectangular gray area 1470 enclosing the descending portion of the pulse 1410 and the second gray area 1480 enclosing the ascending portion of the pulse 1410. The stick model check 1230 (FIG. 12) then normalizes the first value by dividing it by the second value. This normalized value is compared with a threshold. A physiological pulse does not differ too much from the stick model at high pulse rates. This is not true at pulse rates much below 150 bpm because of the appearance of a dicrotic notch and other “bumps.” Hence, the threshold is a function of pulse rate. In one embodiment, the threshold is:

$$0.15, \quad \text{for pulse rate} < 130 \quad (3)$$

$$0.430455769e^{-0.008109302(\text{pulse rate})}, \quad \text{for } 130 < \text{pulse rate} < 160 \quad (4)$$

$$0.1, \quad \text{for pulse rate} > 160 \quad (5)$$

Shown in FIG. 12 is the angle check 1240. The angle check 1240 is based on computing the angle of a normalized slope for the ascending portion of a pulse. This angle is compared with the same angle of an ideal pulse having the same period. This check is effective in discarding pulses that are extremely asymmetric.

FIG. 15 illustrates an example of the angle check 1240 (FIG. 12). Shown is a single triangular pulse 1500 superimposed on the corresponding input waveform 1502. The ascending pulse portion 1504 has a vertical rise  $a$  1510 and a horizontal run  $b$  1520. The rise 1510 and run 1520 are normalized with respect to the pulse signal strength  $ss$  1530 and the pulse frequency, which is 62.5 Hz. in this particular embodiment. An angle  $\theta$  1540 is computed as:

$$\theta = \arctan[(a/ss)/(b/62.5)] \times 180/\pi \quad (6)$$

The angle  $\theta$  is compared with the same angle of an ideal pulse having the same period, where  $a$  is equal to the signal strength and  $b$  is equal to the period  $c$  1550 minus 6.

Three degrees are added to this value as a threshold margin. Hence,  $\theta$  is compared to

5  $\theta_{\text{ref}}$  computed as follow:

$$\theta_{\text{ref}} = \arctan\{[a/ss]/[(c-6)/62.5]\} \times (180/\pi) + 3 \quad (7)$$

If  $\theta < \theta_{\text{ref}}$ , then the pulse is discarded. FIG. 16 illustrates an example pulse 1600 that would be discarded by the angle check, because the segment  $a$  1610 is much smaller than the signal strength  $ss$  1630.

10 Also shown in FIG. 12 is the ratio check 1250. The ratio check component removes pulses in which the ratio between the duration of the ascending pulse portion and the duration of the descending pulse portion is less than a certain threshold. In a particular embodiment, the threshold is 1.1. The rationale for this check is that in every physiological pulse the ascending portion is slower than the descending portion, which  
15 represents the ventricular contraction.

FIG. 17 illustrates an example pulse 1700 that would be discarded by the ratio check 1250 (FIG. 12). In this example, the duration  $a$  1760 of the ascending portion 1710 is less than the duration  $b$  1770 of the descending portion 1720. Hence, the ratio of the ascending duration 1760 to the descending duration 1770,  $a/b$ , is less than the  
20 threshold 1.1.

FIG. 12 further shows the signal strength check 1260. The signal strength check 1260 assigns a confidence value to each pulse, based on its signal strength. There are two levels of confidence, high and low. The determination of confidence is based on two mechanisms. The first mechanism is founded on the observation that the higher the  
25 pulse rate, the lower the signal strength. This mechanism is implemented with an empirical relationship between pulse rate and signal strength. If the measured signal strength is greater than this empirical relationship by a fixed margin, the pulse confidence is low. The second mechanism incorporates the physiological limitation that signal strength cannot change too much over a short period of time. If the pulse signal  
30 strength is greater than a short-term average signal strength by a fixed margin, the pulse

confidence is low. If the pulse meets both criteria, then the pulse has a high confidence. All pulses in a single waveform segment or snapshot have the same confidence value. Hence, if there is a least one pulse with a high confidence, then all pulses with a low confidence will be dropped.

FIG. 18 illustrates the first signal strength criteria described above. In one embodiment, the relationship between signal strength and pulse rate is given by curve 1800, which is described by the following equation:

$$SS = 110.00003722e^{-0.02130936PR} + 1 \quad (8)$$

First, the pulse rate, PR 1810, is determined from the pulse period. Next, the corresponding signal strength,  $SS_{ref}$  1820, is determined from equation (8) and the pulse rate 1810. Because equation (8) is empirically derived, it is shifted up and down to make it more applicable for individual patients. A long-term average signal strength, Long Time SS 1830, and a long-term average pulse rate, Long Time PR 1840, are derived. If Long Time SS 1830 is above the curve 1800 at the point corresponding to the Long Time PR 1840, then the difference between the Long Time SS and the curve 1800 plus 2 becomes Offset 1850. If the measured pulse signal strength, Pulse SS, is less than  $SS_{ref} + \text{Offset}$  1860, then this check is passed.

As shown in FIG. 4, after the candidate pulse subprocessor 410 and the plethysmograph model subprocessor 460, the pulse recognition processor 400 has identified inside the input waveform snapshot all of the pulses that meet a certain model for physiologically acceptable plethysmographs. From the information about these pulses, the pulse statistics subprocessor 490 can extract statistics regarding the snapshot itself. Two useful statistical parameters that are derived are the median value of the pulse periods and signal strengths. The median is used rather than the mean because inside a waveform snapshot of 400 points (almost 7 seconds) the period and signal strength associated with each pulse can vary widely. Another parameter is the signal strength confidence level, which in one embodiment is the same for all the recognized pulses of a snapshot. A fourth useful parameter is pulse density. Pulse density is the value obtained by dividing the sum of the periods of the acceptable pulses by the length of the snapshot. Pulse density represents that ratio of the snapshot that has been

classified as physiologically acceptable. Pulse density is a value between 0 and 1, where 1 means that all of the snapshot is physiologically acceptable. In other words, pulse density is a measure of whether the data is clean or distorted, for example by motion artifact.

5           Finally, based on these described criteria, a pulse rate may be chosen. In a system with additional monitoring inputs, as depicted in FIG. 19, a pulse rate selection and comparison module **1900** may be provided. For example, the oximeter pulse rate (and corresponding confidence information if desired) can be provided on a first input **1902**. In a multiparameter patient monitor, there may also be pulse rate or pulse  
10           information (and possibly confidence information) from an ECG or EKG monitor on a second input **1904**, from a blood pressure monitor on a third input **1906**, from an arterial line on a fourth input **1908**, and other possible parameters **1910**, **1912**. The pulse rate module **1900** then compares the various inputs, and can determine which correlate or which correlate and have the highest confidence association. The selected pulse rate is  
15           then provided on an output **1914**. Alternatively, the pulse rate module **1900** may average each input, a selection of the inputs or provide a weighted average based on confidence information if available.

          The plethysmograph pulse recognition processor has been disclosed in detail in connection with various embodiments of the present invention. These embodiments are  
20           disclosed by way of examples only and are not to limit the scope of the present invention, which is defined by the claims that follow. One of ordinary skill in the art will appreciate many variations and modifications within the scope of this invention.



WHAT IS CLAIMED IS:

1. A processor having a plethysmograph waveform input and a pulse recognition output providing information regarding pulses within said waveform input, said processor comprising:

5 a candidate pulse portion that determines a plurality of potential pulses within said waveform input; and

a physiological model portion that determines the physiologically acceptable ones of said pulses.

10 2. The processor of Claim 1 further comprising a portion that determines statistics of pulses with said waveform input.

3. The processor of Claim 2 wherein one of said statistics is the density of physiologically acceptable pulses within said waveform input.

4. The processor of Claim 1 wherein said candidate pulse portion provides an output identifying said potential pulses as the peaks and valleys of a triangular wave.

15 5. The processor of Claim 1 wherein said physiological model portion comprises a component that extracts features of said potential pulses.

6. The processor of Claim 5 wherein said features include at least one of pulse period, pulse starting point and pulse signal strength.

20 7. The processor of Claim 1 wherein said physiological model portion comprises a component that disregards ones of said potential pulses having a period below a predetermined threshold.

8. The processor of Claim 1 wherein said physiological model portion comprises a component that disregards ones of said potential pulses that are generally asymmetric.

25 9. The processor of Claim 1 wherein said physiological model portion comprises a component that disregards ones of said potential pulses that have a descending trend that is generally slower than a subsequent ascending trend.

10. The processor of Claim 1 wherein said physiological model portion comprises a component that disregards ones of said potential pulses that do not

sufficiently comply with an empirical relationship between pulse rate and pulse signal strength.

11. The processor of Claim 1 wherein said physiological model portion comprises a component that disregards ones of said potential pulses having a signal strength that differs from a short-term average signal strength by greater than a predetermined amount.

12. A method of recognizing pulses within a plethysmograph waveform comprising the steps of:

identifying a plurality of potential pulses in said waveform; and  
10 comparing said potential pulses to a physiological pulse model to derive at least one physiologically acceptable pulse.

13. The method of Claim 13 comprising the further step of generating statistics for said at least one acceptable pulse.

14. The method of Claim 14 wherein said generating step comprises the steps of:

determining a total period of said at least one acceptable pulse;  
calculating the ratio of said total period to a duration of said waveform to derive pulse density.

15. The method of Claim 13 where said comparing step comprises the steps of:

extracting pulse features from said potential pulses; and  
checking said features against a plurality of pulse criteria.

16. A pulse recognition processor comprising:  
a candidate pulse subprocessor means for identifying potential pulses in an input waveform and providing a triangular waveform output;

a plethysmograph model subprocessor means for determining physiologically acceptable pulses in said triangular waveform output and providing as a pulse output the indices of acceptable pulses.

17. The pulse recognition processor of Claim 17 further comprising a pulse statistics subprocessor means for determining cumulative pulse characteristics from said pulse output.

## PLETHYSMOGRAPH PULSE RECOGNITION PROCESSOR

### Abstract of the Disclosure

An intelligent, rule-based processor provides recognition of individual pulses in a pulse oximeter-derived photo-plethysmograph waveform. Pulse recognition occurs in two stages. The first stage identifies candidate pulses in the plethysmograph waveform. The candidate pulse stage identifies points in the waveform representing peaks and valleys corresponding to an idealized triangular wave model of the waveform pulses. At this stage, waveform features that do not correspond to this model are removed, including the characteristic dicrotic notch. The second stage applies a plethysmograph model to the candidate pulses and decides which pulses satisfies this model. This is done by first calculating certain pulse features and then applying different checks to identify physiologically acceptable features. Various statistics can then be derived from the resulting pulse information, including the period and signal strength of each pulse and pulse density, which is the ratio of the analyzed waveform segment that has been classified as physiologically acceptable.

H:\DOCS\SCJ\SCJ-2370.DOC  
120699

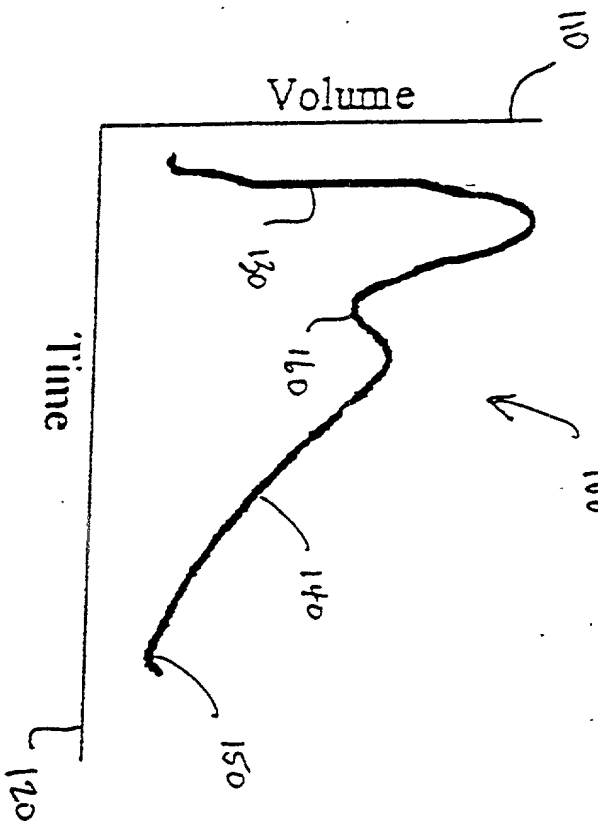


FIG. 1

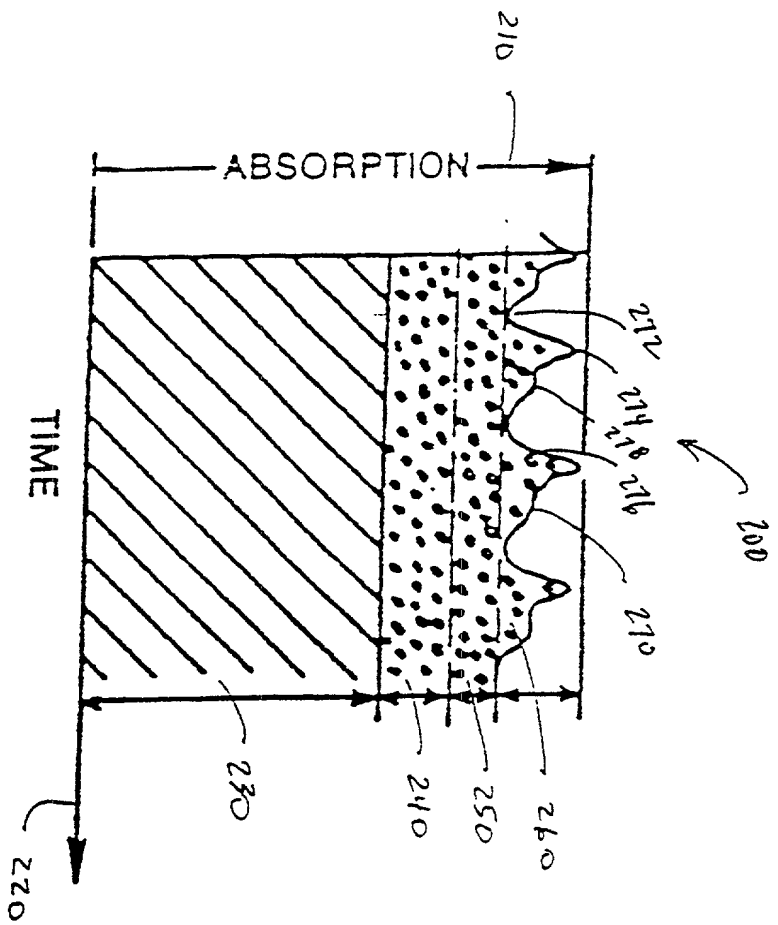
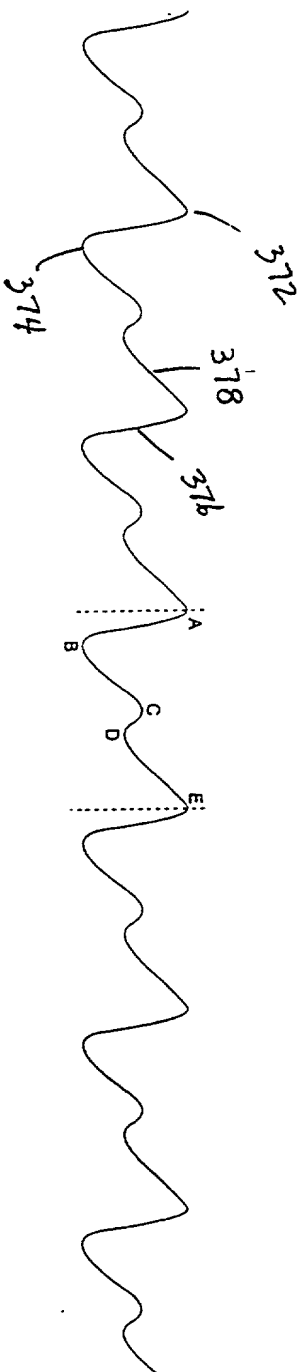


FIG. 2

300



FILE 6.03.12.22.22.22

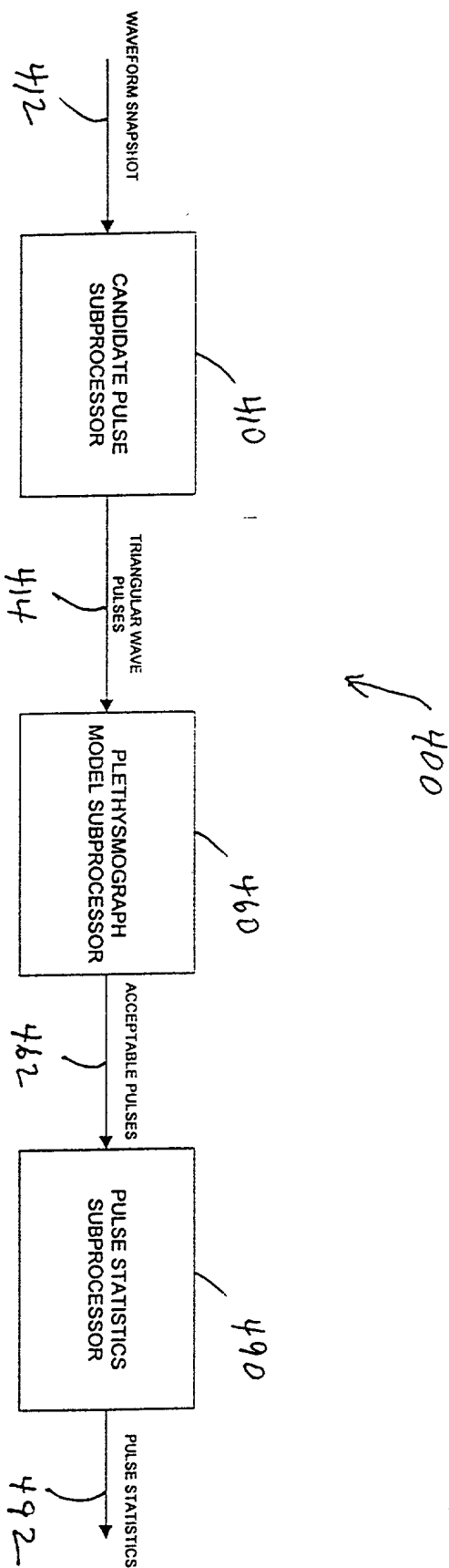


FIG. 4



410

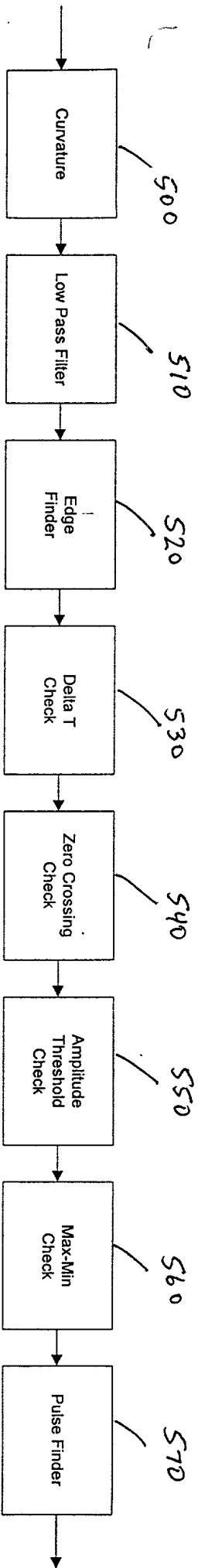
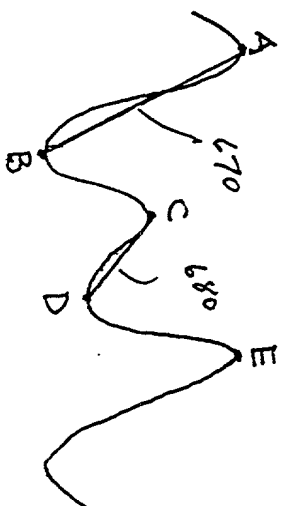


FIG. 5

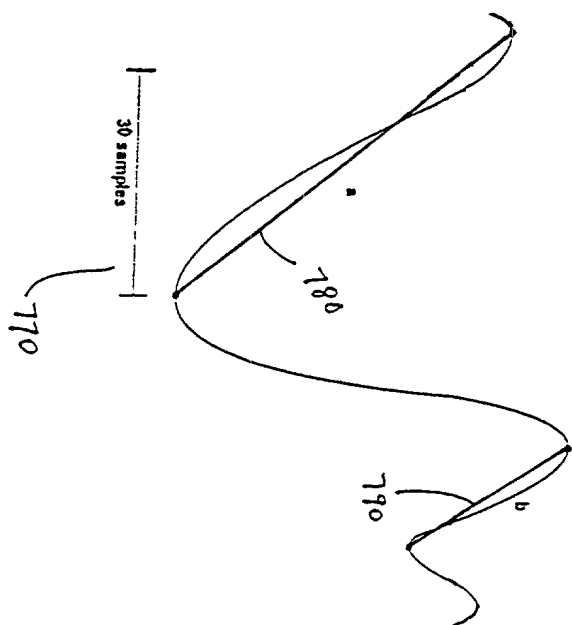


660 →

FIG. 6

094474540 4 24 28 29 30

05410100-72249



760 →

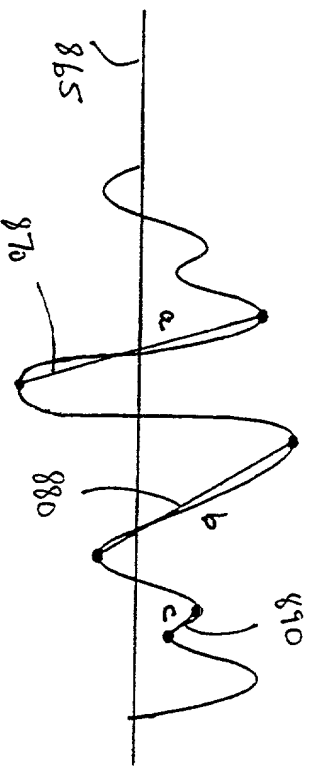


FIG. 8

0044510-122399

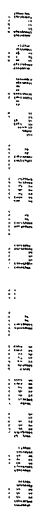


FIG. 9

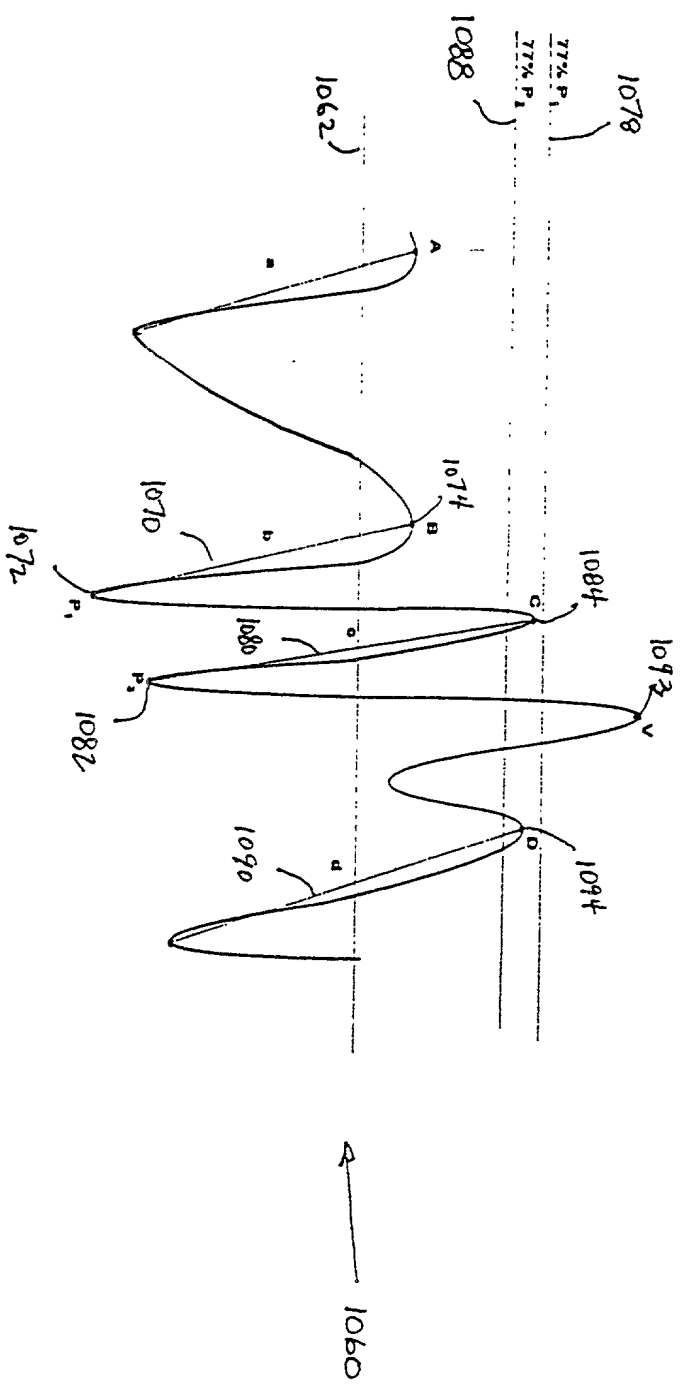


FIG. 10

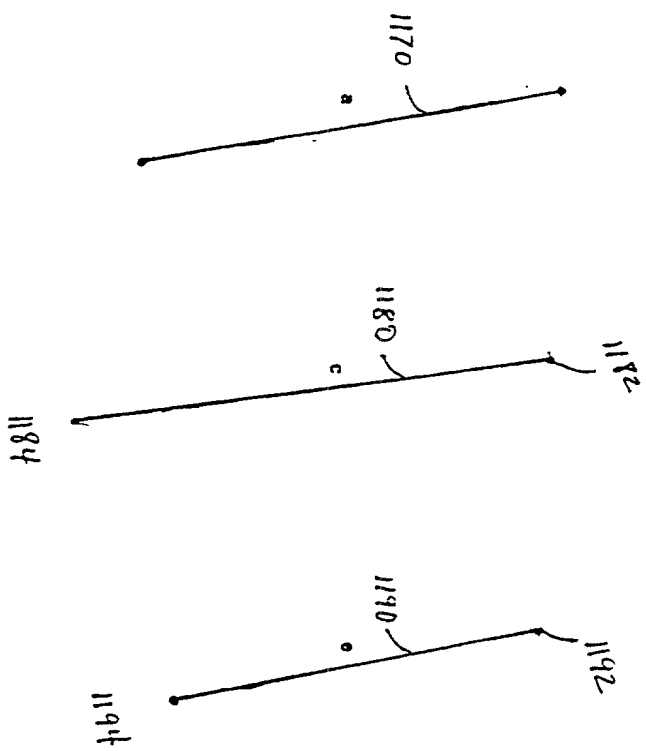
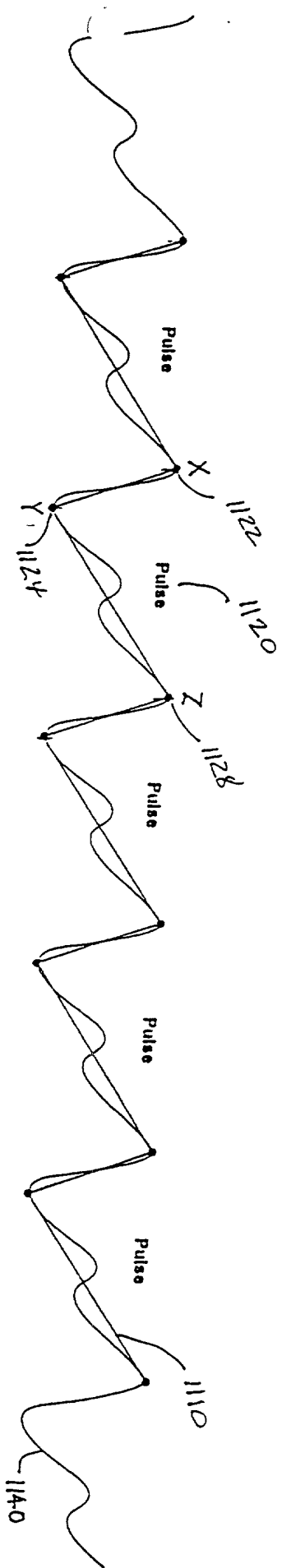
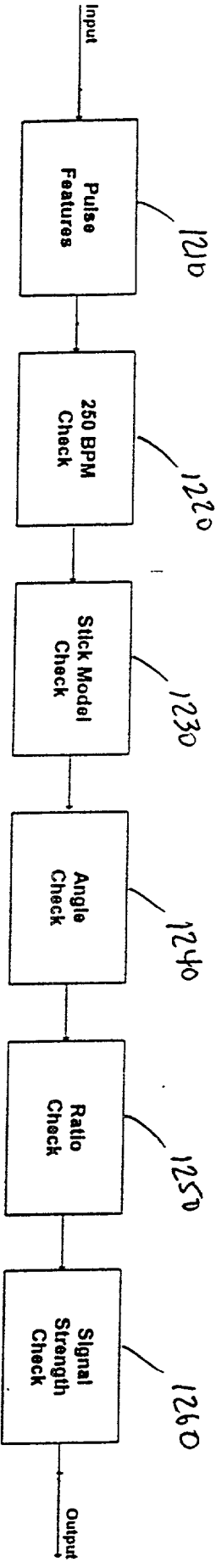


FIG. 11



460

FIG. 12



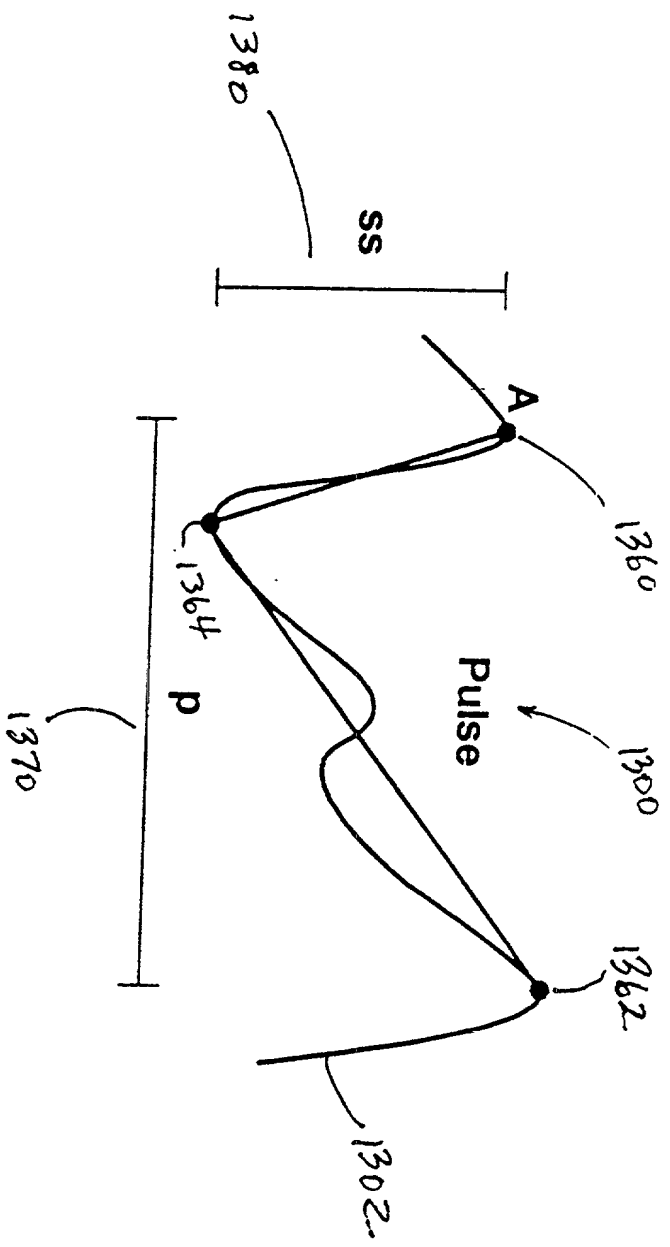


FIG. 13

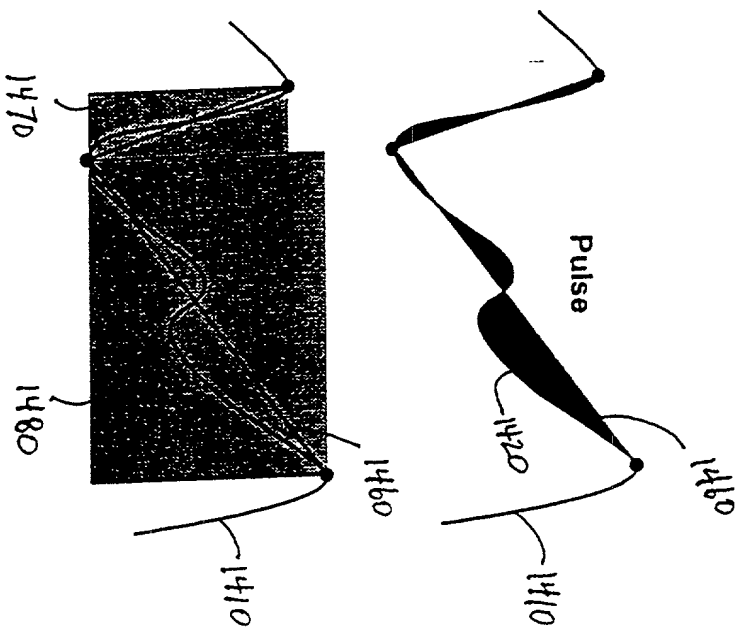
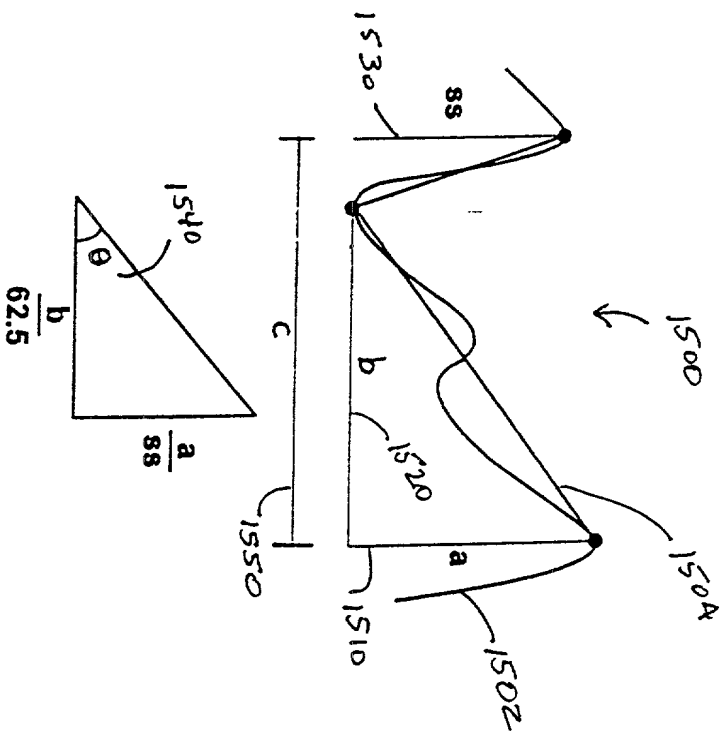


FIG. 14



FTG. 15. 123300

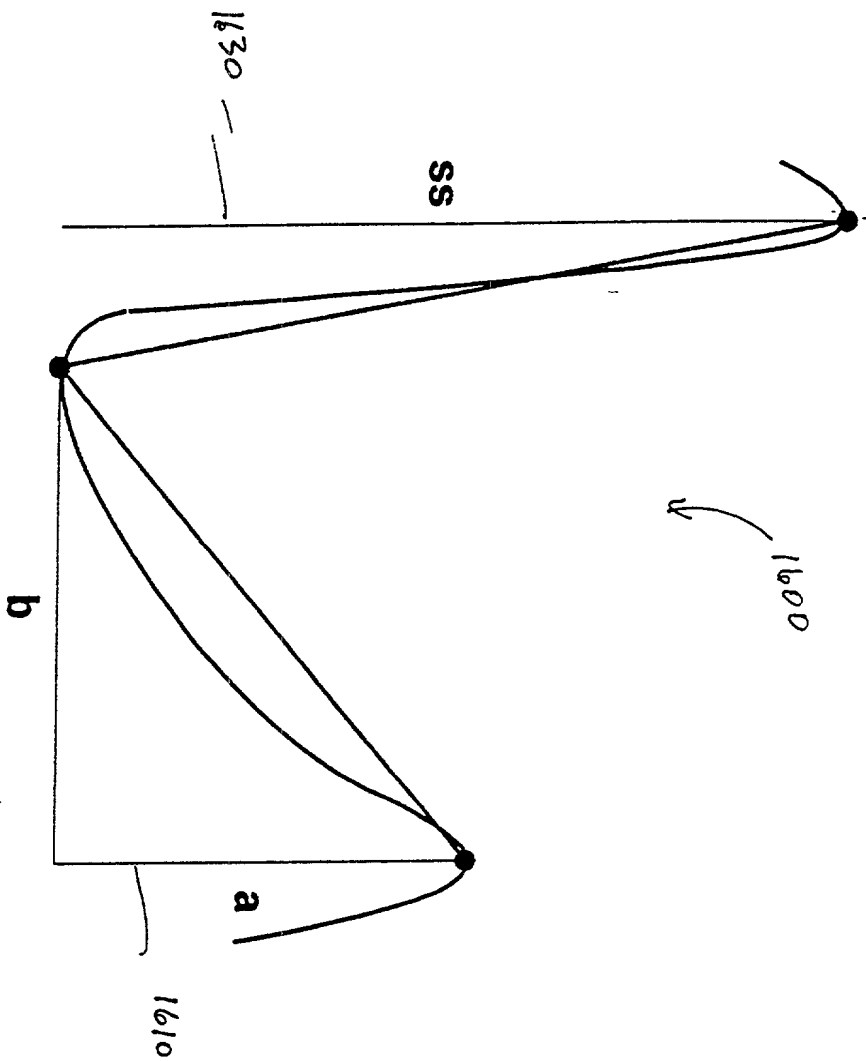


FIG. 16

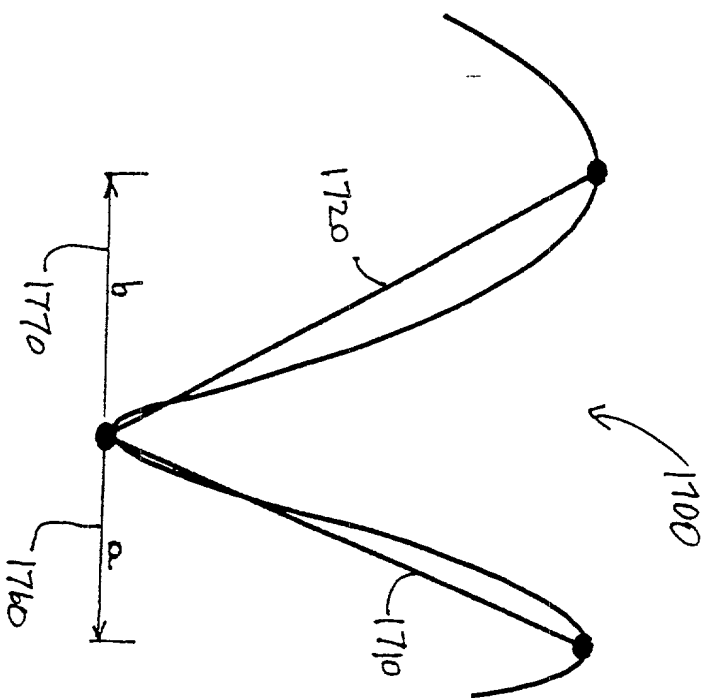


FIG. 17

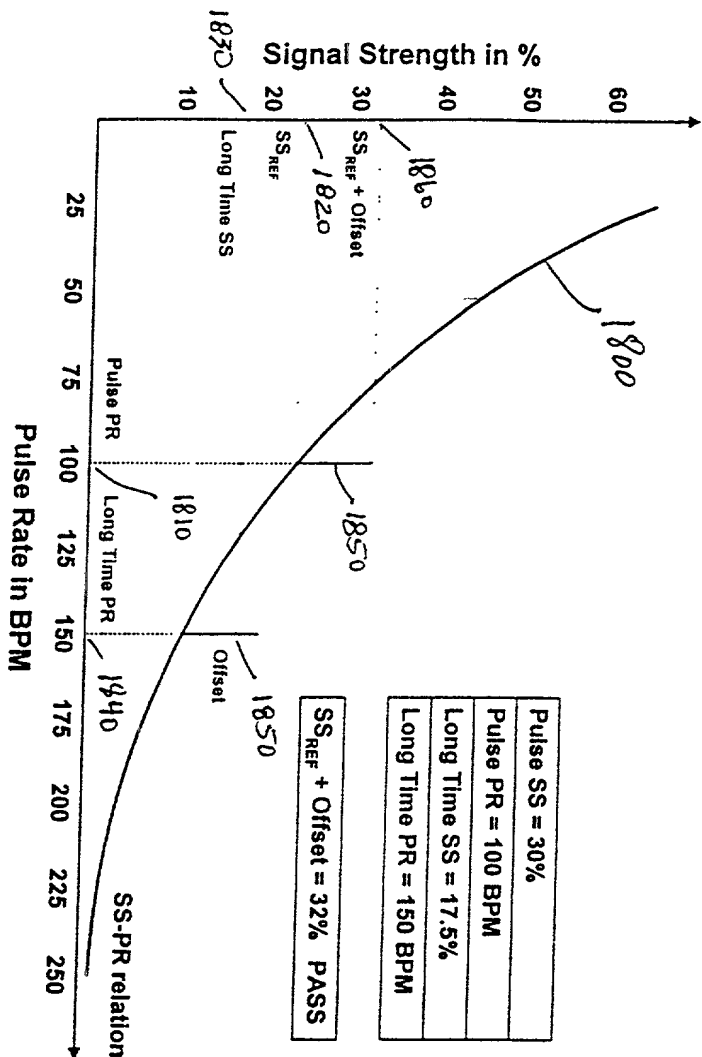


FIG. 18

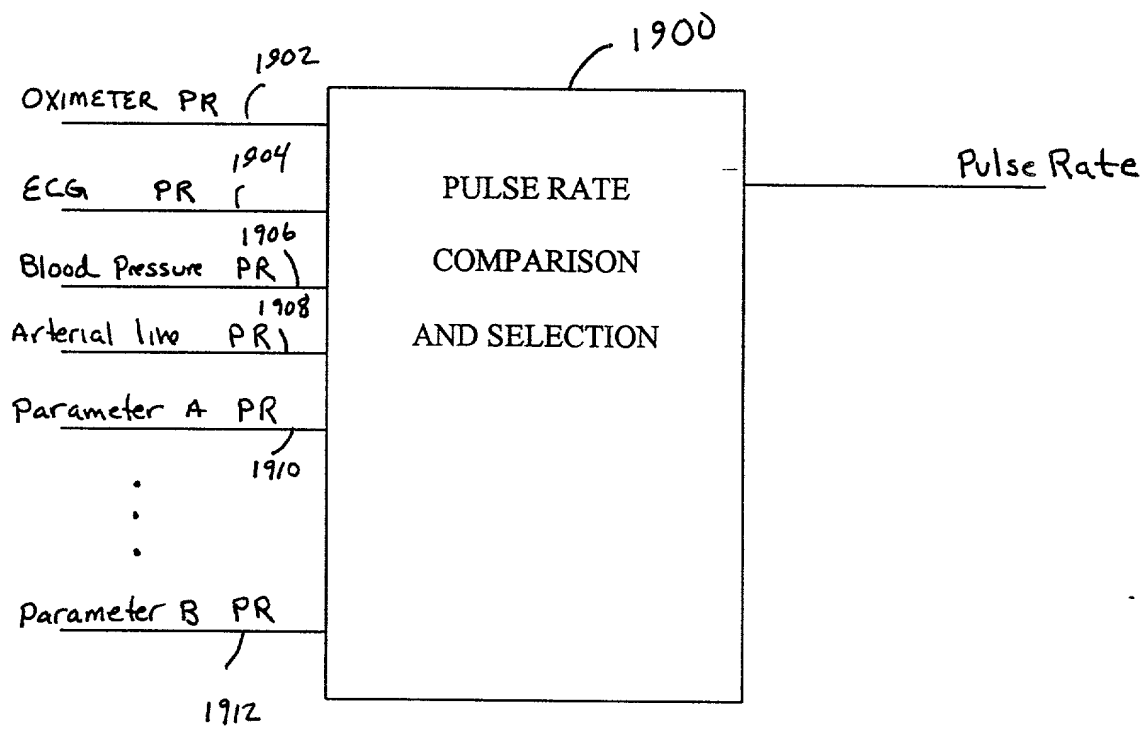


FIG. 19